

RESEARCH COMMUNICATION

Antitumor Activity of Histone Deacetylase Inhibitor Trichostatin A in Osteosarcoma Cells

Dong-Dong Cheng¹, Qing-Cheng Yang^{1*}, Zhi-Chang Zhang¹, Cui-Xia Yang², Yi-Wen Liu²

Abstract

Background: Histone deacetylase (HDAC) inhibitors have been reported to induce cell growth arrest, apoptosis and differentiation of tumor cells. The present study aimed to examine the effects of trichostatin A (TSA), one such inhibitor, on the cell cycle, apoptosis and invasiveness of osteosarcoma cells. **Methods:** MG-63 cells were treated with TSA at various concentrations. Then, cell growth and apoptosis were determined by 3-(4, 5-dimethyl-2-thiazolyl)-2H-tetrazolium bromide (MTT) and TUNEL assays, respectively; cell cycling was assessed by flow cytometry; invasion assays were performed with the transwell Boyden Chamber system. **Results:** MTT assays revealed that TSA significantly inhibited the growth of MG-63 cells in a concentration and time dependent manner. TSA treated cells demonstrated morphological changes indicative of apoptosis and TUNEL assays revealed increased apoptosis of MG-63 cells after TSA treatment. Flow cytometry showed that TSA arrested the cell cycle in G1/G2 phase and annexin V positive apoptotic cells increased markedly. In addition, the invasiveness of MG-63 cells was inhibited by TSA in a concentration dependent manner. **Conclusion:** Our findings demonstrate that TSA inhibits the proliferation, induces apoptosis and inhibits invasiveness of osteosarcoma cells *in vitro*. HDAC inhibitors may thus have promise to become new therapeutic agents against osteosarcoma.

Keywords: Osteosarcoma - trichostatin A - cell cycle - apoptosis - invasiveness

Asian Pacific J Cancer Prev, **13**, 1395-1399

Introduction

Osteosarcoma is the most common primary bone cancer. Although great advances have been achieved in the surgical techniques and new adjuvant chemotherapy, the prognosis of osteosarcoma is still poor and >30% of patients may die of pulmonary metastases within 5 years. As in other neoplasms, genetic factors play a fundamental role in the development of osteosarcoma. Acetylation and deacetylation of histones can alter the chromatin structure by influencing histone-DNA interaction (Wolffe et al., 2000). Acetylation levels of histones are regulated by a dynamic equilibrium between acetylation by histone acetyltransferases (HAT) and deacetylation by histone deacetylases (HDAC), which determines the transcriptional status of chromatin (Ghizzoni et al., 2011). Deacetylated histones have been found to be associated with cell growth, whereas hyperacetylated histones with cell growth arrest, differentiation and/or apoptosis. The aberrant recruitment of HDAC complex that represses the transcription of specific genes such as tumor suppressor genes may lead to transcriptional regulation (Marks et al., 2001).

HDAC inhibitors are known to cause growth arrest,

differentiation or apoptosis of cancer cells including human breast cancer cells, prostate cancer cells, lung cancer cells, ovary cancer cells and colon cancer cells (Vigushin et al., 2001; Donadelli et al., 2003; Kim et al., 2003; Chiba et al., 2004). The HDAC inhibitor, trichostatin A (TSA), was initially characterized as an anti-fungal drug and later found to inhibit HDAC activity at nanomolar concentrations (Yoshida et al., 1995). TSA has been suggested to block the catalytic reaction by chelating a zinc ion in the active site pocket through its hydroxamic acid group (Finnin et al., 1999). The anti-proliferative effect of TSA has been demonstrated in some malignancies; however, it has not been well studied in osteosarcoma cells. So, in the present study, we aimed to investigate the effects of TSA on the growth, apoptosis and invasiveness of human osteosarcoma MG-63 cells.

Materials and Methods

Cell Culture

The osteosarcoma MG-63 cells were purchased from the ATCC (CRL-1427). MG-63 cells were maintained in an atmosphere with 5% CO₂ at 37°C in Dulbecco's modified Eagle's medium (DMEM) containing 4 mM

¹Department of Orthopedics, ²Laboratory Center, the Sixth People's Hospital, Shanghai JiaoTong University, Shanghai, China
*For correspondence: tjqc@163.com

L-glutamine, 1.5 g/L sodium bicarbonate, 4.5 g/L glucose and 1.0 mM sodium pyruvate, 10% fetal bovine serum (FBS) and 1% penicillin/ streptomycin (Invitrogen).

TSA Treatment

TSA was purchased from Sigma, dissolved in dimethyl sulfoxide (DMSO) (3 mM) and stored at -80°C for use. Twenty-four hours before TSA addition, MG-63 cells were subcultured onto either fresh tissue culture plates. When the cell confluence reached 60-70%, the medium was replaced with fresh medium containing TSA at various concentrations (10~500 nm/ml), and incubation was performed for 12, 24 and 48 h. Then, cells were harvested, washed with phosphate buffered saline (PBS) twice, and examined for TSA-induced changes.

Assessment of Cell Viability and Cell Growth Inhibition

The cells were seeded in 96-well plates and maintained in DMEM containing 10% FBS and TSA at various concentrations. Cells were harvested at different time points and cell growth was determined. Cells were stained with trypan blue and then counted using a hemacytometer. Cell proliferation was examined by using the 3-(4, 5-dimethyl- 2-thiazolyl)-2H-tetrazolium bromide (MTT) assay as previously described (Mosmann, 1983).

Morphological changes in MG-63 cells exposed to TSA

Morphological changes in MG-63 were examined after TSA treatment by using a phase contrast microscope and an electron microscope. The suspended cells were removed and the ultrastructure of adherent cells was examined. In brief, cells were fixed in 2.5% glutaraldehyde, and then in 1% osmium tetroxide, dehydrated in a series of ethanol, embedded in epoxy resin, and examined under an electron microscope (JEM 1200EX).

Detection of Apoptotic Cells

Quantification of apoptotic cells was performed by the terminal deoxynucleotidyl transferase mediated dUTP biotin nick end labeling (TUNEL) according to the manufacturer's instructions (Takara Bio Inc.). Cells grown on coverslips were washed twice with PBS, fixed in 4% paraformaldehyde and treated with 3% H₂O₂ for 20 min. After washing with PBS, cells were further incubated with streptavidin HRP solution for 30 min at room temperature and stained with 3, 3'-diaminobenzidine tetrahydrochloride (DAB, 0.05%). Then, these cells were washed, and stained with hematoxylin for 1 min. A total of 4 fields were randomly selected from each section at a magnification of ×400 and the TUNEL-positive cells were calculated. The proportion of apoptotic cells was calculated as the ratio of the number of positive cells to total cell numbers.

Detection of Cell Cycle and Apoptosis by Flow Cytometry

The percentage of cells in G₁, S and G₂/M phase was determined by flow cytometry. Briefly, cells were digested with trypsin, washed once in fresh media, and re-suspended at a density of 1×10⁶ cells/ml. The cell suspension (200 μl) was then incubated with PI solution (50 μg/ml) and 50 units of RNase for 30 min. The stained cell nuclei were determined on an Epixs XL flow

cytometer (Beckman Coulter). Data were analyzed using the Multicycle software which allowed a simultaneous estimation of cell cycle parameters.

In addition, cells were washed twice with cold PBS, and 1×10⁶ cells were re-suspended in binding buffer. FITC conjugated Annexin V was added at a final concentration of 1 μg/ml. PI was added at a final concentration of 0.25 μg/ml. Then, these cells were gently vortexed and incubated at room temperature for 15 min in the dark. FITC positive cells were determined by flow cytometry within 30 min.

Invasion Assay

Matrigel (B.D. Biosciences) is a soluble basement membrane matrix. Invasion assay of MG-63 cells was performed with a transwell Boyden Chamber (Corning Life Sciences) carrying a polycarbonate filter with a pore size of 8-μm, which was precoated with Matrigel at 50 μg/mL. The lower chamber was filled with 0.6 ml of serum-free medium containing 0.1% FBS. Cells were re-suspended at a density of 1.5×10⁶ cells/mL with TSA or vehicle (DMSO) in serum-free medium containing 0.1% FBS and 10 ng/ml VEGF. Then, 100 μL of cell suspension and 200 μL of serum-free medium containing 0.1% BSA were added to the upper chamber, followed by incubation for 12 h at 37°C. Cells on the upper filter were removed by wiping, and then the filter was fixed in 4% paraformaldehyde for 1 h. Cells passing through the filter were stained with 1% crystal violet. Following washings with PBS, the filters were treated with 2% sodium dodecylsulfate (SDS) overnight and the optical density (OD) was determined at 490 nm. The invasiveness inhibition was determined as follow: invasiveness inhibition = [1 - (ODTSA-ODblank) / (ODcontrol-ODblank)]×100% (Li et al., 2004).

Statistical analysis

Three independent experiments were carried out and means ± standard deviations (SD) calculated. Student t test was employed for comparisons. A value of P less than 0.05 were considered statistically significant.

Results

Inhibitory Effects of TSA on Osteosarcoma Cell Proliferation

Our results showed TSA inhibited the proliferation of osteosarcoma cells. MTT assay revealed TSA inhibited the growth of MG-63 cells in concentration and time dependent manners (Figure 1). The inhibition rate after 300 nM TSA treatment was 86% at 12 h, 67% at 24 h and 56% at 48 h. Cell viability at 48 h after treatment with TSA at 50, 100, 200, 300 and 500 nm was 78%, 65%, 56% and 46%, respectively.

Morphological Changes in Osteosarcoma Cells after Exposure to TSA

Phase contrast microscopy demonstrated that MG-63 cells exposed to TSA exhibited morphological changes including cytoplasmic elongation (round) and loss of cell-cell contact (detached). These morphological changes

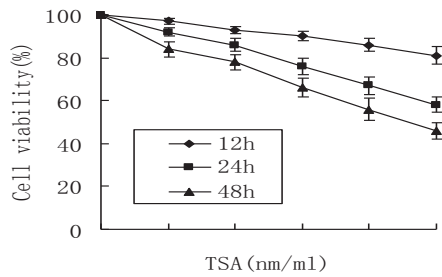


Figure 1. Cell Growth after TSA Treatment. MG-63 cells were exposed to TSA at various concentrations for 12, 24 and 48 h. TSA inhibited the growth of MG-63 cells in concentration and time dependent manners

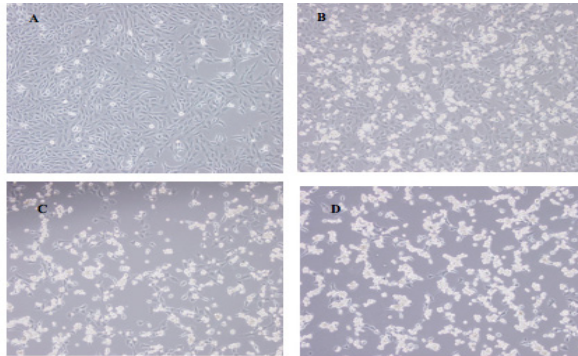


Figure 2. Phase-contrast Microscopy of MG-63 Cells after TSA Treatment. MG-63 cells were treated with vehicle or TSA at 300 nm for 12 h, 24 h and 48 h. The morphology of these cells were observed under an inverted phase contrast microscope. TSA-treated cells became round and detached. A: vehicle. B: TSA treatment for 12 h. C: TSA treatment for 24 h. D: TSA treatment for 48 h ($\times 100$)

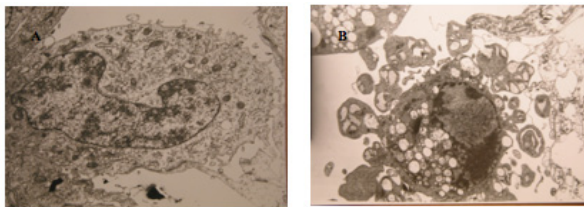


Figure 3. Ultrastructure of MG-63 Cells after TSA Treatment. A: vehicle. B: TSA treatment. The apoptotic features included a paucity of cytoplasmic organelles, vacuoles, condensation of the chromatin, and numerous apoptotic bodies ($\times 3000$)

appeared to be concentration and time dependent (Figure 2). Ultrastructurally, cells were shrunken with a paucity of cytoplasmic organelles, vacuoles, nuclear shrinking accompanied by margination and condensation of the chromatin, and presence of numerous apoptosis bodies (Figure 3). These morphological features were indicative of apoptosis.

Apoptosis after TSA Treatment

The TUNEL staining demonstrated the increase of apoptotic MG-63 cells after TSA treatment, which was concentration and time dependent (Figure 4). About 75% of cells appeared to be dead after 300 nM TSA treatment for 24 h. Apoptosis was not noted in untreated cells. The apoptosis peaked at 48 h after 300 nM TSA treatment.

Cell Cycle and Apoptosis by Flow Cytometry

The cell cycle of MG-63 cells was analyzed at 24 h

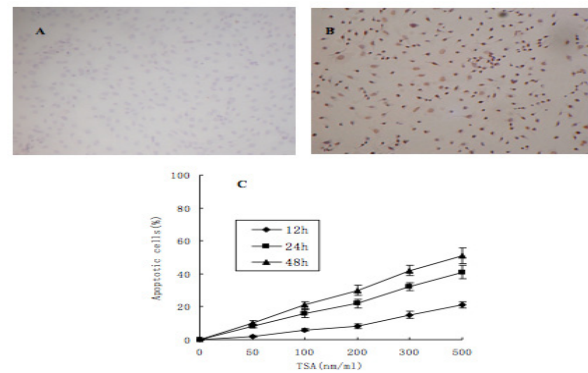


Figure 4. Detection of Apoptosis of MG-63 Cells after TSA Treatment with TUNEL Staining. A: untreated cells. Apoptosis was not found ($\times 400$). B: Cells after 300 nM TSA treatment for 24 h ($\times 400$). C: TSA increased the apoptotic MG-63 cells in a concentration and time dependent manners

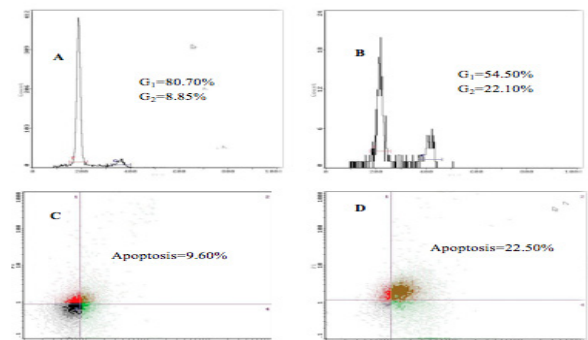


Figure 5. Detection of Cell Cycle and Apoptosis of MG-63 Cells after TSA Treatment by Flow Cytometry. Cells were treated with the vehicle (A, C) or 300 nM TSA for 24 h (B, D). Flow cytometry showed a marked decrease in cells with dual peaks and an increase in cells in the G2/M phase (A, B). Annexin V staining showed an increase in the apoptotic cells after TSA treatment (C, D)

after exposure to 300 nM TSA. Flow cytometry after PI staining demonstrated dual peaks before TSA treatment. Figure 5A showed that the proportion of untreated cells was 80.70% in G1 phase and 8.85% in G2/M phase. As shown in Figure 5B, the percentage of TSA-treated cells in G0/G1 phase was markedly decreased but that in G2/M phase dramatically increased (22.10%). This meant that the cell cycle progression was arrested by TSA. Annexin V staining was used to measure the TSA induced apoptosis. The lower right quadrant represents the apoptotic cells. FITC-Annexin V positive apoptotic cells increased gradually from 9.60% in untreated cells to 22.50% at 24 h after 300 nM TSA treatment (Figure 5 C, D).

TSA inhibits osteosarcoma cell invasiveness

The invasiveness of cancer cells into Matrigel has been used to characterize the involvement of extracellular matrix receptors and degrading enzymes, which play a role in cancer progression and thus to characterize the malignant potential of cancer cells. Invasion assay showed a large number of cells passed through the filter in the control group (Figure 6 A), whereas the cells passing through the filter were markedly reduced after 300 nM TSA treatment (Figure 6B). Moreover, the TSA reduced the number of invasive cells in a concentration dependent manner (Figure 6C) ($P < 0.05$).

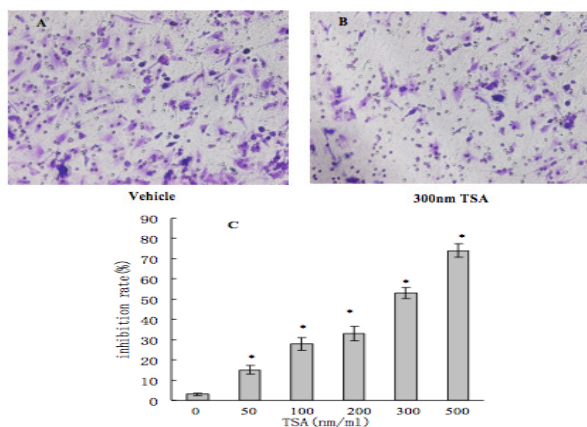


Figure 6. Invasiveness of MG-63 Cells after TSA Treatment. Cell invasiveness was determined after TSA treatment by using the transwell system. A: vehicle (DMSO). B: Treatment with 300 nM TSA ($\times 400$). C: TSA inhibited the invasiveness of MG-63 cells in a concentration dependent manner. * $P < 0.05$

Discussion

The acetylation level of histone is reversibly regulated by HAT and HDAC (Ghizzoni et al., 2011). An inappropriate acetylation state of histones causes abnormal outgrowth and the altered pattern of cell death, which leads to neoplastic transformation (Loidl et al., 1987). Regulation of angiogenic factor expression through histone acetylation has been found to be involved in the angiogenesis (Williams, 2001). Studies have shown that over-expression of HDAC1 may induce angiogenesis both in vitro and in vivo through increasing VEGF expression and suppressing p53 and VHL expressions (Kim et al., 2001). These findings suggest that HDAC plays an important role in the angiogenesis which is closely related to carcinogenesis. Although TSA has been reported to inhibit cell growth and induce apoptosis of various cancer cells, its effect on osteosarcoma cells is rarely investigated.

In the present study, MTT assay revealed that TSA could inhibit the growth of osteosarcoma cells in concentration and time dependent manners. The morphological changes in osteosarcoma cells after TSA treatment were similar to those following treatment with anti-cancer drugs. Anticancer agents have been demonstrated to induce apoptosis of different cancer cells (Muller et al., 1997). To determine whether the reduction and morphological changes in osteosarcoma cells after TSA treatment were as results of increase in apoptotic cells, the apoptosis of osteosarcoma cells was further examined. TUNEL staining showed that TSA significantly induced the apoptosis of osteosarcoma cells, which may be partially attributed to the growth inhibition of osteosarcoma cells.

The exact mechanism by which TSA induced apoptosis of osteosarcoma cells is still unknown, as is the mechanism of apoptosis after treatment with anti-cancer drugs. Further investigations are required.

To determine whether TSA affected the distribution of cell cycle, cell nuclei were stained with PI and examined by flow cytometry. Results indicated that TSA markedly reduced the osteosarcoma cells in G1 phase and concomitantly increased those in G2/M phase. Annexin V

staining revealed the increase of apoptotic cells after TSA treatment. It has been found that TSA can result in growth arrest in G1 and/or G2/M phase and induce apoptosis of a variety of cancer cells (Strait et al., 2002; Hirose et al., 2003). The arrest in G1 phase after TSA treatment is thought to be related to the increased expressions of p21/WAF1, while the precise mechanism causing arrest in G2/M phase or apoptosis following TSA treatment in cancer cells still remains to be elucidated (Sowa et al., 1997). The findings in morphological examination including the electron microscopy, TUNEL staining and flow cytometry were indicative of apoptosis after TSA treatment and demonstrated that TSA could inhibit the proliferation of osteosarcoma cells in vitro. Our results indicate that TSA is capable of inducing growth arrest by facilitating apoptosis and arresting cell cycle in G1/G2 phase.

Invasiveness is a very important characteristic of cancer cells and closely related to matrix metalloproteinases (MMPs). Previous study shows TSA suppresses the invasiveness of lung cancer cells by activating RECK expression and attenuating MMP-2 activity (Liu et al., 2003). As shown in Figure 6, our results demonstrated that TSA significantly reduced the number of cells penetrating the filter in cell invasion assay.

Taken together, our findings demonstrate the anti-tumor effect of HDAC inhibitors and they may become new therapeutic agents for the treatment of osteosarcoma. However, further in vivo studies are required to confirm the effectiveness and safety of TSA in the treatment of human osteosarcoma.

Acknowledgements

We thank He Yi-qing for technical assistance in flow cytometry and Ren Jia-qiang for helpful suggestions in TUNEL assay. This study was supported by the National Natural Science Foundation of China (No. 30973017).

References

- Aquerreta I, Aldaz A, Giraldez J, Sierrasesumaga L (2004). Methotrexate pharmacokinetics and survival in osteosarcoma. *Pediatr Blood Cancer*, **42**, 52-8.
- Chiba T, Yokosuka O, Fukai K, et al (2004). Cell growth inhibition and gene expression induced by the histone deacetylase inhibitor, trichostatin A, on human hepatoma cells. *Oncology*, **66**, 481-91.
- Donadelli M, Costanzo C, Faggioli L, et al (2003). Trichostatin A, an inhibitor of histone deacetylases, strongly suppresses growth of pancreatic adenocarcinoma cells. *Mol Carcinog*, **38**, 59-69.
- Finnin MS, Donigian JR, Cohen A, et al (1999). Structures of a histone deacetylase homologue bound to the TSA and SAHA inhibitors. *Nature*, **401**, 188-93.
- Ghizzoni M, Haisma HJ, Maarsingh H, Dekker FJ (2011). Histone acetyltransferases are crucial regulators in NF- κ B mediated inflammation. *Drug Discov Today*, **16**, 504-11.
- Hirose T, Sowa Y, Takahashi S, et al (2003). p53-independent induction of Gadd45 by histone deacetylase inhibitor: coordinate regulation by transcription factors Oct-1 and NF-Y. *Oncogene*, **22**, 7762-73.

- Kim MS, Kwon HJ, Lee YM, et al (2001). Histone deacetylases induce angiogenesis by negative regulation of tumor suppressor genes. *Nat Med*, **7**, 437-43.
- Kim Y, Park H, Lim Y, et al (2003). Decreased syndecan-2 expression correlates with trichostatin-A induced-morphological changes and reduced tumorigenic activity in colon carcinoma cells. *Oncogene*, **22**, 826-30.
- Li MH, Miao ZH, Tan WF, et al (2004). Pseudolaric acid B inhibits angiogenesis and reduces hypoxia-inducible factor 1alpha by promoting proteasome-mediated degradation. *Clin Cancer Res*, **10**, 8266-74.
- Liu LT, Chang HC, Chiang LC, Hung WC (2003). Histone deacetylase inhibitor up-regulates RECK to inhibit MMP-2 activation and cancer cell invasion. *Cancer Res*, **63**, 3069-72.
- Loidl P, Grobner P (1987). Postsynthetic acetylation of histones during the cell cycle: a general function for the displacement of histones during chromatin rearrangements. *Nucleic Acids Res*, **15**, 8351-66.
- Marks PA, Richon VM, Breslow R, Rifkind RA (2001). Histone deacetylase inhibitors as new cancer drugs. *Curr Opin Oncol*, **13**, 477-83.
- Mosmann T (1983). Rapid colorimetric assay for cellular growth and survival: application to proliferation and cytotoxicity assays. *J Immunol Methods*, **65**, 55-63.
- Muller M, Strand S, Hug H, et al (1997). Drug-induced apoptosis in hepatoma cells is mediated by the CD95 (APO-1/Fas) receptor/ligand system and involves activation of wild-type p53. *J Clin Invest*, **99**, 403-13.
- Sowa Y, Orita T, Minamikawa S, et al (1997). Histone deacetylase inhibitor activates the WAF1/Cip1 gene promoter through the Sp1 sites. *Biochem Biophys Res Commun*, **241**, 142-50.
- Strait KA, Dabbas B, Hammond EH, et al (2002). Cell cycle blockade and differentiation of ovarian cancer cells by the histone deacetylase inhibitor trichostatin A are associated with changes in p21, Rb, and Id proteins. *Mol Cancer Ther*, **1**, 1181-90.
- Vigushin DM, Ali S, Pace PE, et al (2001). Trichostatin A is a histone deacetylase inhibitor with potent antitumor activity against breast cancer in vivo. *Clin Cancer Res*, **7**, 971-6.
- Williams RJ (2001). Trichostatin A, an inhibitor of histone deacetylase, inhibits hypoxia-induced angiogenesis. *Expert Opin Investig Drugs*, **10**, 1571-3.
- Wolffe AP, Guschin D (2000). Review: chromatin structural features and targets that regulate transcription. *J Struct Biol*, **129**, 102-22.
- Yoshida M, Horinouchi S, Beppu T (1995). Trichostatin A and trapoxin: novel chemical probes for the role of histone acetylation in chromatin structure and function. *Bioessays*, **17**, 423-30.